EUROPHYSICS LETTERS 1 January 2006

Europhys. Lett., **73** (1), pp. 135–141 (2006)
DOI: 10.1209/epl/i2005-10351-4

Controlled DNA compaction within chromatin: The tail-bridging effect

F. Mühlbacher[1], C. Holm[1,2] and H. Schiessel[1,3]

[1] *Max-Planck-Institut für Polymerforschung, Theory Group PO Box 3148, D-55021 Mainz, Germany*
[2] *FIAS, JW Goethe-Universität - Max-von-Laue Strasse 1 D-60438 Frankfurt/Main, Germany*
[3] *Instituut-Lorentz, Universiteit Leiden - Postbus 9506 2300 RA Leiden, The Netherlands*

received 26 August 2005; accepted in final form 27 October 2005
published online 23 November 2005

PACS. 87.15.He – Dynamics and conformational changes.
PACS. 87.16.Sr – Chromosomes, histones.
PACS. 36.20.Ey – Conformation (statistics and dynamics).

Abstract. – We study a mechanism underlying the attraction between nucleosomes, the fundamental packaging units of DNA inside the chromatin complex, by introducing a simple model of the nucleosome: the eight-tail colloid, a negatively charged sphere with eight oppositely charged, flexible, grafted chains that represent the terminal histone tails. We demonstrate that our complexes are attracted via the formation of chain bridges and that this attraction can be tuned by changing the fraction of charged monomers on the tails. This suggests a physical mechanism of chromatin compaction where the degree of DNA condensation can be controlled via biochemical means, namely the acetylation and deacetylation of lysines in the histone tails.

Introduction. – In eukaryotes (plants and animals) meters of DNA have to be compacted inside micron-sized nuclei. At the same time a considerable fraction of the genetic code has to be accessible. Nature has solved this formidable task by compacting DNA in a hierarchical fashion [1]. The first step consists of wrapping the DNA two turns around cylinders made from eight histone proteins. This leads to a string of cylindrical DNA spools about 10 nm in diameter and 6 nm in height, each repeating unit being called a nucleosome [2]. The chromatin fiber with diameter of about 30 nm is typically posited as the next compaction level which again forms higher-order structures such as loops. The density of such structures varies along the fiber and in the course of the cell-cycle and is presumably directly related to the genetic activity with the dense regions corresponding to "silenced" parts.

It is far from being obvious how nature copes with the challenge of combining high compaction and (selective) accessibility at the same time. Recently —via the combination of experiments and theory— an understanding has begun to emerge of how the nucleosome is meticulously designed to face this challenge. In principle, when DNA is wrapped onto the protein cylinder, it is in a "closed" state not accessible for DNA binding proteins. But thermal

fluctuations open a window of opportunity for such proteins via the unwrapping of either one of the two turns [3, 4] or via a corkscrew sliding of the octamer *along* the DNA chain [5, 6]. Also remodelling complexes can actively induce nucleosome sliding along DNA [7].

Less clear, however, is the situation at the next levels of compaction. The chromatin fiber has a roughly 40 times shorter contour length than that of the DNA chain it is made from. But at the same time the fiber is much stiffer than the naked chain, so that its coil size in dilute solution would still be much larger than the diameter of the cell nucleus [8]. This clearly calls for the necessity of nucleosome-nucleosome attraction as a further means of compaction, a mechanism that needs to be tunable such that fractions of the fiber are dense and transcriptionally passive, while others are more open and active.

This leads to several important questions: Can nucleosomes attract each other, and what, if so, is the underlying mechanism? Can this interaction be tuned for individual nucleosomes? And can this all be understood in simple physical terms? Recent experiments indeed point towards a simple mechanism that leads to attraction between nucleosomes: the histone tail bridging [11–13]. The histone tails are flexible extensions of the eight core proteins that carry several positively charged residues [2, 14]. These tails extend considerably outside the globular part of the nucleosome. Mangenot *et al.* [11] studied dilute solutions of nucleosome core particles (NCPs; the particles that are left when the non-adsorbed "linker" DNA is digested away). Via small-angle X-ray scattering it was demonstrated that NCPs change their size with salt concentration: At around 50 mM monovalent salt the radius of gyration increases slightly (from 43 Å to 45 Å), but at the same time the maximal extension of the particle increases significantly (from 140 Å to 160 Å). This observation was attributed to the desorption of the cationic histone tails from the NCP, which carries an overall negative charge (cf. ref. [1]). Osmometric measurements [12] detected around the salt concentration where the tails desorb an attractive contribution to the interaction between the NCPs, manifest in a considerable drop of the second virial coefficient. The coincidence of the ionic strengths for the two effects led Mangenot *et al.* to suggest that it is the tails that are mainly involved in the attractive interaction [15]. This picture was recently supported by another study [13] where it was shown that the attraction disappeared after the tails on the NCPs had been removed.

On the theoretical side the role of histone tails is not clear. Attraction between simplified model nucleosomes has been reported [17,18], yet this model ignored the tails. The nucleosome was modelled by a positively charged sphere (representing the protein core) and a semiflexible cationic chain (the DNA) wrapped around. The interaction between two such complexes (at zero temperature) showed an attraction at intermediate salt concentrations leading to a non-monotonic behavior of the second virial coefficient with a minimum reflecting that attractive regime (cf. fig. 4 in [17]). On the other hand, Podgornik [19] focused on tail bridging in a model where the NCP was represented by a point-like particle with an oppositely charged flexible chain. This system showed NCP-NCP attraction but no non-monotonic behavior of the second virial coefficient. Thus the question arises whether it is really the tail bridging that causes the attraction between NCPs observed at intermediate salt concentrations.

Another possible mechanism for the attraction could be based on correlations between charge patches [20]. An example provides a recent computer simulation of Allahyarov *et al.* [21] who studied the interaction between spherical model proteins decorated with charge patches; the second virial coefficient featured a non-monotonic behavior as a function of ionic strength. Also the non-monotonic interaction found by Boroudjerdi and Netz [17] can be interpreted to belong to this class of attraction induced by charge correlations.

Strong theoretical support that tails are important in the interaction between nucleosomes within a chromatin fiber comes from a very recent computer simulation [22] where the NCP crystal structure has been mimicked by a cylinder with 277 charge patches (accounting for

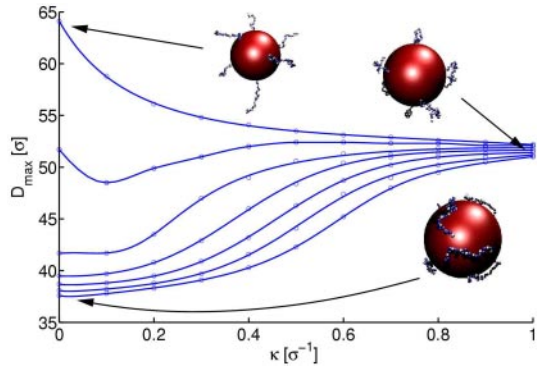

Fig. 1 – Average maximal extension of the eight-tail colloid as a function of the salt concentration together with three example configurations. The different curves correspond to different values of the central charge: $|Z| = 0, 50, 100, 150, 200, 250, 300$ (from top to bottom).

charged groups on the surface of the NCP) with all the tails anchored to it. By switching on and off the charges on the tails it was found that the tails play a crucial role in the electrostatic nucleosome-nucleosome and nucleosome-linker DNA interaction within that chromatin fiber model —causing the stabilization of the fiber at physiological salt conditions. Even though this study shows the importance of tails for nucleosomal interaction, it does not reveal what is really the underlying physical mechanism.

The purpose of the present study is fourfold: i) to introduce a minimal model for an NCP including its tails, ii) to test whether such a model shows attraction with a non-monotonically varying second virial coefficient, iii) to put tail bridging on a stronger footing and demonstrate that this effect is qualitatively different from attraction through charge patches, and iv) to demonstrate how tail bridging can be used to facilitate control of the compaction state of chromatin.

Model. – We start with presenting our NCP model, the eight-tail colloid depicted in fig. 1. It consists of a sphere with eight attached polymer chains. The sphere is a coarse-grained representation of the NCP without the tails, *i.e.*, the globular protein core with the DNA wrapped around. The sphere carries a central charge Z that represents the net charge of the DNA-octamer complex; since the DNA overcharges the cationic protein core, one has $Z < 0$ [1]. Furthermore, the sphere radius is chosen to be $a = 15\sigma$ with $\sigma = 3.5$ Å being our unit length. The eight histone tails are modelled by flexible chains grafted onto the sphere (at the vertices of a cube). Each chain consists of 28 monomers of size σ where each third monomer carries a positive unit charge, the rest being neutral. All these parameters have been chosen to match closely the values of the NCP [23]. The simulations were performed in a NVT ensemble, using a Langevin thermostat [25] with a time step of 0.01 τ, and a friction coefficient $\Gamma = \tau^{-1}$ (Lennard-Jones time unit). The hard cores were modelled with a purely repulsive Lennard-Jones potential [26], the chain connectivity with a finitely extensible non-linear elastic (FENE) potential [26], and the central sphere was allowed to freely rotate (cf. ref. [24] for details of the implementation). In addition, all charged monomers and the central sphere experience an electrostatic interaction via the standard Debye-Hückel (DH) theory with an inverse screening length $\kappa = \sqrt{4\pi l_B c_s}$, where c_s denotes the monovalent salt concentration and $l_B = 2\sigma$ sets the Bjerrum length in water at room temperature ($l_B = e^2/\epsilon k_B T$, e: electron charge, ϵ: dielectric constant of solvent, $k_B T$: thermal energy) [27]. Since we use a DH potential, we need to use

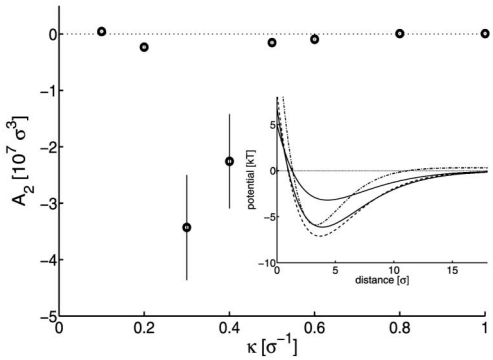

Fig. 2 – Second virial coefficient of the eight-tail colloid as a function of salt concentration. The inset shows the interaction potential between two eight-tail colloids as a function of the surface-surface separation for 4 different values of κ: $\kappa\sigma = 0.2$ (dash-dotted line), $\kappa\sigma = 0.3$ (dashed line), $\kappa\sigma = 0.4$ (solid line) and $\kappa\sigma = 0.6$ (top solid grey line).

an effective value $Z_{\rm eff}$ for the central charge to account for charge renormalization [28].

Results and discussion. – Figure 1 presents results of a Molecular Dynamics (MD) simulation of a single eight-tail colloid. Depicted is the thermally averaged maximal extension of the colloid as a function of κ for different values of the central sphere charge Z. For $Z = 0$ and small values of κ, *i.e.*, at low ionic strength, the eight tails are extended, radially pointing away from the center of the complex, cf. the example at $\kappa\sigma = 0$. For large values of $|Z|$, say, for $|Z| > 100$, and small κ the tails are condensed onto the sphere, cf. the configuration at $|Z| = 300$ and $\kappa\sigma = 0$. Increasing the screening leads in both cases finally to structures where the chains form random polymer coils as the ones in the example at $\kappa\sigma = 1$. With increasing values of $|Z|$ the swelling of initially condensed tails sets in at larger κ-values. A comparison of our curves for $|Z| > 100$ with the experimental ones [11] shows a qualitatively similar chain unfolding scenario. Furthermore, by choosing $Z = -150$ we are able to match closely the experimental and the simulation values of c_s at which tail unfolding takes place. In the following we will therefore always use this value as our $Z_{\rm eff}$.

We determined next the interaction between two such complexes by measuring the thermally averaged force at different distances and by interpolating the force-distance curve via a suitable least-square fit. Integration then yields the pair potentials depicted in the inset of fig. 2 for four different values of κ. We find an attractive potential with a minimum of a few k_BT in all four cases. The depth of the potential shows a non-monotonic dependence on κ with a maximal value around $\kappa\sigma = 0.3$. This in turn is reflected in a non-monotonic dependence of the second virial coefficient A_2 (cf. fig. 2) with a minimum around the κ-value where tail unfolding occurs, cf. the curve for $Z = Z_{eff} = -150$ in fig. 1. Again, all these observations are qualitatively similar to the experimental ones [12].

Having a simulation model at hand allows us now to determine whether this attraction can be attributed to the tail-bridging effect. In fig. 3 we depict a comparison of the full eight-tail model with simplified variants. In all cases we choose $\kappa\sigma = 0.4$, a value close to the one where A_2 has its minimal value in Fig. 2; $\kappa\sigma = 0.4$ corresponds to 100 mM monovalent salt, *i.e.*, to physiological conditions. In one case (top right) we collapse each chain on a small patch modelled as a grafted monomer that carries the whole chain charge [29]. Inspecting the attractive part of the pair potential, we see that this patch model has a very rapidly decaying interaction with a slope larger than the reference line with slope κ. In sharp contrast, the

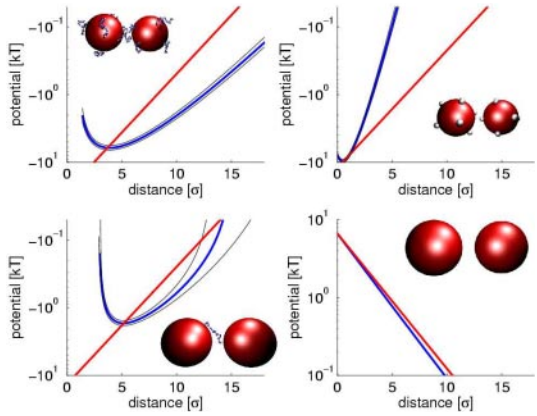

Fig. 3 – Comparison of the interaction potential (with error corridor) for 4 different colloids at $\kappa\sigma = 0.4$: eight-tail colloids (top left), colloids with charge patches (top right), one-tail bridging (bottom left) and homogeneously charged balls (bottom right). For each model we depict the potential in a semilogarithmic plot (only the attractive part for the three first cases). The curves are compared to a line with slope $\pm\kappa$.

eight-tail complex has a decay constant that is smaller than κ (cf. top left of fig. 3), an effect that can only be attributed to tail bridging. This effect can also be seen for our third variant (bottom left) where 15 of the 16 tails have been removed and Z has been adjusted so that the net charges of the complexes are unchanged. The remaining one-tail complex is not allowed to rotate so that the grafting point of the chain always faces the other ball. Also in that case the range of attraction is longer than expected from pure screened electrostatics. Finally, on the bottom right we present the trivial case of two charged balls (with the same net charge as

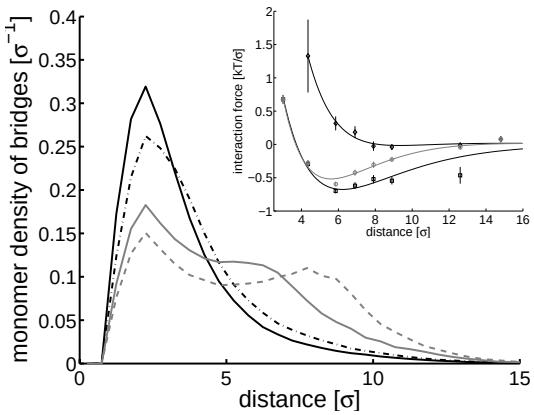

Fig. 4 – Density distribution of monomers belonging to bridge-forming tails as a function of the distance from the surface of the colloid to which the tail is grafted. The different distributions correspond to different surface-surface separations between colloids: $d = 0\sigma$ (solid), $d = 4\sigma$ (dash-dotted), $d = 7\sigma$ (grey) and $d = 9\sigma$ (dashed). The inset separates the total average of the interaction force (circles) into the part stemming from configurations with bridges (squares) and non-bridging configurations (diamonds).

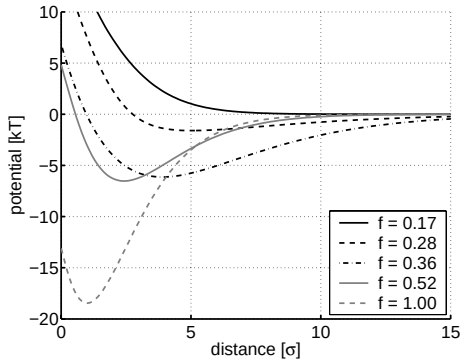

Fig. 5 – Interaction potential between two eight-tail complexes as a function of the surface-surface separation for $\kappa\sigma = 0.4$ and various charge fractions f.

the full model) where only a *repulsive* interaction remains.

Having established the qualitative difference between tail-induced attraction and attraction via charge patches we take in fig. 4 a closer look at the tail-bridging effect between two eight-tail colloids, again for $\kappa\sigma = 0.4$. Depicted is the monomer distribution of bridge-forming chains. We define such a chain as a chain that has at least one of its monomers closer than a distance 3.6σ to the surface of the alien core. For very small distances between the colloids there are almost always bridges. Their monomer distribution shows a strong peak around a distance 3σ. However, also at much larger distances like $d = 7\sigma$ and $d = 9\sigma$ there is still a considerable fraction of configurations that show bridges. Their monomer distribution shows a bimodal distribution with the two peaks clearly reflecting the condensation of monomers on the home core and the alien core. The inset shows the interaction force between two colloids (circles) and the contributions of tail-bridging configurations (squares) and configurations without bridges (diamonds) to this force. It can be clearly seen that the tail-bridging configurations account to an overall attractive force, whereas in the other case the interaction is on average purely repulsive.

Finally, we speculate how the tail bridging can be used by the cellular machinery to control DNA compaction and genetic activity. We have determined the pair potential between eight-tail complexes for different charge fractions of the tails. As can be seen in fig. 5, its equilibrium distance goes to larger values and finally disappears when one goes from a charge fraction $f = 0.36$ (the value used above) to $f = 0.17$. It is in fact known that the cellular machinery is capable of controlling the charge state of the histone tails via the acetylation (the "discharging") and deacetylation (the "charging") of its lysine groups [30]. Active, acetylated regions in chromatin are more open, inactive, deacetylated regions tend to condense locally and on larger scales as well [31]. For instance, chromatin fibers tend to form hairpin configurations once a sufficiently strong internucleosomal attraction has been reached [10, 32]. This suggests a biochemical means by which the degree of chromatin compaction and genetic activity can be controlled via a physical mechanism, the tail-bridging effect.

* * *

The authors thank M. Deserno, B. Dünweg, K. Kremer, F. Livolant, S. Mangenot and R. Podgornik for helpful discussions.

REFERENCES

[1] Schiessel H., *J. Phys. Condens. Matter*, **15** (2003) R699.
[2] Luger K., Mader A. W., Richmond R. K., Sargent D. F. and Richmond T. J., *Nature*, **389** (1997) 251.
[3] Polach K. J. and Widom J., *J. Mol. Biol.*, **254** (1995) 130.
[4] Kulic I. M. and Schiessel H., *Phys. Rev. Lett.*, **92** (2004) 228101.
[5] Gottesfeld J. M., Belitsky J. M., Melander C., Dervan P. B. and Luger K., *J. Mol. Biol.*, **321** (2002) 249.
[6] Kulic I. M. and Schiessel H., *Phys. Rev. Lett.*, **91** (2003) 148103; Mohammad-Rafiee F., Kulic I. M. and Schiessel H., *J. Mol. Biol.*, **344** (2004) 47.
[7] Becker P. B., *EMBO J.*, **21** (2002) 4749.
[8] The size of a stiff polymer chain in a good solvent scales like $R \approx l_P^{1/5} D^{1/5} L^{3/5}$ (l_P: persistence length, D: diameter, L contour length) [9]. A human chromosomal DNA chain has $L \approx 4\,\mathrm{cm}$. This together with $l_P = 50\,\mathrm{nm}$ and $D \approx 4\,\mathrm{nm}$ (assuming physiological ionic conditions) leads to $R \approx 100\,\mu\mathrm{m}$. On the other hand the chromatin fiber has $L \approx 1\,\mathrm{mm}$, $l_P \approx 200\,\mathrm{nm}$ [10] and $D \approx 30\,\mathrm{nm}$ leading to $R \approx 20\,\mu\mathrm{m}$. Note that there are 46 chains that have to fit into the nucleus with a diameter of 3 to $10\,\mu\mathrm{m}$.
[9] Odijk T. and Houwaart A. C., *J. Polym. Sci.*, **16** (1978) 627.
[10] Mergell B., Everaers R. and Schiessel H., *Phys. Rev. E*, **70** (2004) 011915.
[11] Mangenot S., Leforestier A., Vachette P., Durand D. and Livolant F., *Biophys. J.*, **82** (2002) 345.
[12] Mangenot S., Raspaud E., Tribet C., Belloni L. and Livolant F., *Eur. Phys. J. E*, **7** (2002) 221.
[13] Bertin A., Leforestier A., Durand D. and Livolant F., *Biochemistry*, **43** (2004) 4773.
[14] Luger K. and Richmond T. J., *Curr. Opin. Gen. Dev.*, **8** (1998) 140.
[15] Note the opposite effect of colloidal stabilization that occurs when polyelectrolyte chains are grafted densely onto colloids, cf. [16].
[16] Pincus P., *Macromolecules*, **24** (1991) 2912.
[17] Boroudjerdi H. and Netz R. R., *Europhys. Lett.*, **64** (2003) 413.
[18] Boroudjerdi H. and Netz R. R., *J. Phys. Condens. Matter*, **17** (2005) S1137.
[19] Podgornik R., *J. Chem. Phys.*, **118** (2003) 11286.
[20] Rouzina I. and Bloomfield V. A., *J. Phys. Chem.*, **100** (1996) 9977.
[21] Allahyarov E., Löwen H., Hansen J. P. and Louis A. A., *Phys. Rev. E*, **67** (2003) 051404.
[22] Sun J., Zhang Q. and Schlick T., *Proc. Natl. Acad. Sci. (U.S.A.)*, **102** (2005) 8180.
[23] We choose here the average length of the N-terminal tails whose lengths range from 15 residues (histone H2A) to 44 (H3). The tail bridging effect reported here is very robust: variations in, *e.g.*, the anchor positions have only a minor impact on the interaction between our complexes [24]. In the context of the cell some tails (the two H3 tails) might be involved in the interaction with the linker DNA thereby controlling the DNA entry-exit angle as detailed in chapter 3.5 of ref. [1].
[24] Mühlbacher F., Schiessel H. and Holm C., in preparation
[25] Frenkel D. and Smit B., *Understanding Molecular Simulation*, 2nd edition (Academic Press, San Diego) 2002.
[26] Kremer K. and Grest G. S., *J. Chem. Phys.*, **92** (1990) 5057.
[27] McQuarrie D. A., *Statistical Mechanics* (Harper-Collins, New York) 1976.
[28] Alexander S., Chaikin P. M., Grant P., Morales G. J., Pincus P. and Hone D., *J. Chem. Phys.*, **80** (1984) 5776.
[29] We note that this model variant also shows a non-monotonic dependence of A_2 on c_s [24] so that this feature is not a criterion to distinguish between tail bridging and attraction via patchiness.
[30] Horn P. J. and Peterson C. L., *Science*, **297** (2002) 1824.
[31] Tse C., Sera T., Wolffe A. P. and Hansen J. C., *Mol. Cell. Biol.*, **18** (1998) 4629.
[32] Grigoryev S. A., Bednar J. and Woodcock C. L., *J. Biol. Chem.*, **274** (1999) 5626.